

The Lifebelt Particle Filter for robust estimation from low-valued count data

Alice Corbella^{1, 2, §}, Trevelyan J. McKinley³, Paul J. Birrell^{4, 2}, Anne M. Presanis^{2, 4}, Simon E. F. Spencer¹, Gareth O. Roberts¹, and Daniela De Angelis^{2, 4}

¹*Department of Statistics, University of Warwick*

²*MRC Biostatistics Unit, University of Cambridge*

³*University of Exeter Medical School, University of Exeter*

⁴*UK Health Security Agency*

[§]*Corresponding author alice.corbella@warwick.ac.uk*

September 2022

Abstract

Particle filtering methods are well developed for continuous state-space models. When dealing with discrete spaces on bounded domains, particle filtering methods can still be applied to sample from and marginalise over the unknown hidden states.

Nevertheless, problems such as particle degradation can arise in this context and be even more severe than they are within the continuous-state domain: proposed particles can easily be incompatible with the data and the discrete system could often result in all particles having weights of zero. However, if the boundaries of the discrete hidden space are known, then these could be used to prevent particle collapse.

In this paper we introduce the Lifebelt Particle Filter (LBPF), a novel method for robust likelihood estimation when low-valued count data arise. The LBPF combines a standard particle filter with one (or more) *lifebelt particles* which, by construction, will tend not to be incompatible with the data. A mixture of resampled and non-resampled particles allows for the preservation of the lifebelt particle, which, together with the remaining particle swarm, provides samples from the filtering distribution, and can be used to generate estimates of the likelihood.

The LBPF can be used within a pseudo-marginal scheme to draw inference on static parameters, θ , governing a discrete state-space model with low-valued counts. We present here the applied case estimating a parameter governing probabilities and timings of deaths and recoveries of hospitalised patients during an epidemic.

1 Introduction

State-space models (SSMs) are stochastic processes that make use of a latent variable representation to describe a dynamical phenomenon (Schön et al., 2018). SSMs are used in disparate fields, from object positioning in engineering (Gilks and Berzuini, 2001; Solin et al., 2018), to evolution of weather conditions (Anderson, 1996), to virus spread in a population (Bretó et al., 2009; Dukic, Lopes, and Polson, 2012). These models, usually Markovian, express (i) the evolution of latent variables over time by means of a *state distribution* $p(\mathbf{X}_t | \mathbf{X}_{t-1}, \theta)$ and (ii) the

generation of data by means of an *observation distribution* $p(\mathbf{Y}_t|\mathbf{X}_t, \boldsymbol{\theta})$. $\boldsymbol{\theta}$ is called the *static parameter(s)* and is usually the main focus of the inference; in the Bayesian setting the goal is often to derive its posterior distribution: $p(\boldsymbol{\theta}|\mathbf{y}_{1:T})$.

Sequential Monte Carlo (SMC) methods are a family of inferential tools that, among other things, are particularly useful for inference in SSMs. Exploiting the Markovian structure of the SSM, SMC enables sampling from the distribution of the latent states conditionally on the data, $p(\mathbf{X}_t|\mathbf{y}_{1:t}, \boldsymbol{\theta})$, often called the *filtering distribution*. The bootstrap particle filter (BPF) is an example of this sequential sampling scheme (Gordon, Salmond, and Smith, 1993). The BPF, in turn, allows the formulation of an exact estimator for the likelihood of the static parameter, i.e. $p(\mathbf{Y}_{1:T}|\boldsymbol{\theta})$. Many references are available for these methods, including a recent volume by Chopin and Papaspiliopoulos (Chopin, Papaspiliopoulos, et al., 2020) and key papers (Arulampalam et al., 2002; Doucet, Johansen, et al., 2009; Schön et al., 2018).

Generating samples from the filtering distribution is key to drawing inference on the parameter $\boldsymbol{\theta}$: samples are obtained by generating a set of particles via sequential use of importance sampling mechanisms. The resulting samples can be embedded, for example, in a Markov chain Monte Carlo (MCMC) algorithm, such as the Metropolis Hastings (MH) algorithm, enabling exact inference of the posterior of interest, $p(\boldsymbol{\theta}|\mathbf{y}_{1:T})$, leading to the family of *pseudo-marginal methods* (Andrieu and Roberts, 2009). Alternatively, they could be embedded in another sequential method that samples from a series of distributions that converge to the target of interest (Chopin, Jacob, and Papaspiliopoulos, 2013). Here we use an SMC approximation of the likelihood within an MCMC algorithm, so-called particle Markov chain Monte Carlo (pMCMC), which was outlined in Andrieu, Doucet, and Holenstein (2010).

For all these methods to work, it is key to have a *good* mechanism to sample from the filtering distribution. Here *good* is defined from an importance-sampling perspective: the closer the proposals for the latent state match the true latent state, the better the estimator of the likelihood will be, and hence the inference. If the particles sampled for the latent state are not consistent with the true filtering distribution, a phenomenon known as *particle degradation* takes place: as the sequential approximation progresses, fewer and fewer particles have a non-negligible importance weight, and therefore the particles become non-representative of the filtering distribution. The most serious outcome is *particle collapse*, which happens when all the particles have weight equal to 0.

This problem is exacerbated in SSMs involving discrete low-valued random variables (r.v.s). Often these systems involve distributions on bounded spaces, such as Binomial or Multinomial r.v.s, either in the state or in the observation distributions: the support of these variables is restricted and it can be very hard to find an importance distribution that covers the support and while proposing values around the mass of the filtering distribution. Another challenging example can be that of Approximate Bayesian Computation (ABC) where the weight is often assigned according to an indicator function (equal to 1 if the synthetic observations are within some distance from the true observations or 0 otherwise), which is also likely to lead to particle collapse in a discrete low-count context. The problem is even more severe when the observation distribution is highly concentrated, leaving little space for importance proposals with weight greater than 0. The *chained* dynamics of many discrete SSMs are the underlying cause of this problem: not only do the particles sampled need to be coherent with the observations at time point t , but also with the future observations, to allow the full run of the importance sampling mechanism from the beginning to the end of the time series. Atypical data and outliers challenge even more these mechanisms, provoking full particle collapse when just one new data point is included after a fairly well-behaved particle set.

Some attempts have been made to extend the basic SMC mechanisms, such as the BPF, to be robust in discrete, low-count systems. The alive particle filter (APF) (Del Moral et al., 2015) is a

SMC method that allows for an unbounded number of particles n_t . The idea behind the algorithm is to keep sampling proposed particles until a desired number of particles N with non-zero weight is obtained. Drovandi, Pettitt, and McCutchan (2016) looked at the application of the APF in the context of low-count data and observed that the algorithm can have potentially an unbounded cost. Even if a limit B can be placed on the computation executed (e.g. by stopping after $L < N$ particles have been observed but $l_t \geq B$ have been evaluated), the APF is likely to take long time to run if the value of θ has low likelihood (Drovandi, Pettitt, and McCutchan (2016), Remark 4) e.g. for parameter proposals towards the tails when a pseudo-marginal mechanism is used. McKinley et al. (2020) exploited much of the potential of the APF in this context, allowing for early rejection of bad values of θ . Despite their efforts and improvements, the authors note that the algorithm remains substantially computationally expensive, preventing its use for longer time series or in contexts where real-time inference is needed.

Griffin et al. (2017) attempts to solve a related problem by considering more general quasi-stationary distributions, i.e. Markov processes with an absorbent state. Griffin et al. (2017) uses SMC samplers to target the Limiting Conditional Distribution of a such a Markov processes; simulated trajectories attain weight 0 if they enter the absorbing state. Their proposed solution acts on the resampling step of the algorithm using regional re-sampling (RRS), which works by dividing the space of the latent variables into regions and reallocating a fixed number of particles between them, thereby reducing the probability of all the weight falling on one particle. Furthermore, zero weight particles are reallocated to high weight locations in “Combine-split resampling,” a resampling technique that improves effective sample size (ESS) with zero variance. Despite this approach, there is still a positive probability of particle collapse and the robustness of the algorithm solely depends on the creation of these regions. Moreover Griffin et al. (2017) considers only SSMs with “static” space while, as shown in the example below, we consider problems where the domain is expanding.

This paper proposes a mechanism to implement a particle filter in the context of low-valued discrete states, that is safer against particle collapse. This is achieved by adopting a mixture of importance distributions each targeting a different scope: some elements of the mixture, the *lifebelt* particles, will be safely sampled from parts of the space that are unlikely to result in zero weights; while the remaining particles will be drawn from a mechanism exploring different parts of the latent space, where the filtering distribution should concentrate, but might result easily in particle collapse. Moreover, we propose a mixture of resampling and non-resampling importance steps so that the safer component of the mixture will always be resampled. This new scheme is named the lifebelt particle filter (LBPF).

While the method proposed can be used in many contexts, the explicit form that the lifebelt particles take is dependent upon to the SSM under analysis. Hence, this paper is guided by the example that initially motivated the design of the LBPF. This is the problem of estimating the hospitalised case fatality risk (hCFR) (i.e. the risk of death given hospitalisation with a specific condition) during epidemics when only time series of the number of hospitalised and dead individuals are provided. Section 2 illustrates this problem in the context of SSMs, discusses its relevance and outlines the inferential challenges. Section 3 proposes the LBPF as a possible solution to the problem of particle collapse in the model outlined; Section 4 reports the results obtained by applying the LBPF within a pseudo marginal method to infer the hCFR. Section 5 compares the LBPF with the APF; lastly Section 6 discusses applicability and draws conclusions.

1.1 Notation

Some notation has already been introduced above. Greek letter are used for static parameters, while Latin letters for dynamic parameters (states and observations); lower case Latin letters are

values and realisations of such states. Many states are indexed by time y_t , where the notation $\mathbf{y}_{1:t}$ indicates vector (y_1, y_2, \dots, y_t) . Table 1 reports many elements used throughout the manuscript.

Symbol	Meaning
$p(\mathbf{X}_t \mathbf{X}_{t-1}, \boldsymbol{\theta})$	state distribution
$p(\mathbf{Y}_t \mathbf{X}_t, \boldsymbol{\theta})$	observation distribution
$p(\mathbf{X}_t \mathbf{y}_{1:t}, \boldsymbol{\theta})$	filtering distribution
$w_t^{(n)}$	un-normalised weight of particle n at time t
$\tilde{w}_t^{(n)}$	self-normalised weight of particle n at time t , so that $\sum_{n=1}^N \tilde{w}_t^{(n)} = 1$

Table 1: SSM and SMC Notation

2 Motivation

2.1 Hospitalised case fatality risk estimation

The estimation of the case fatality risk (CFR), i.e. the probability of death given a disease, is particularly crucial for emerging epidemics: the timely availability of estimates for the risk of death for different case-definitions (e.g. hospitalised case fatality risk, hCFR, symptomatic case fatality risk, sCFR) can provide valuable information for a health-policy response.

Time series on the number of cases at different levels of severity are usually collected during the emergence of a new epidemic and through subsequent monitoring. Nevertheless, only outcomes of higher severity (e.g. appearance of symptoms, hospitalization, death) are usually reported, while positive outcomes (e.g. disappearance of symptoms, recovery, discharge from hospital) are rarely monitored.

We consider, the situation when counts of confirmed cases admitted to hospital and confirmed deaths in hospital are recorded. This is the situation for influenza in England: the UK Severe Influenza Surveillance System (USISS; Health Protection Agency, 2011), now replaced by the SARI Watch survey (UK Health Security Agency, 2021), collects the weekly number of cases admitted to intensive care and deaths with confirmed influenza.

Let y_t and h_t denote the number of confirmed deaths and hospitalisations that happened during time interval t , respectively. Estimators of the CFR based on cumulative-counts such as $\widehat{CFR}_t = \frac{\sum_{t=1}^T y_t}{\sum_{t=1}^T h_t}$ are still commonly employed, as they do not require any information in addition to the two time series $\mathbf{y}_{1:T}$ and $\mathbf{h}_{1:T}$ (World Health Organization (WHO), 2015). Nevertheless, they are well known to be affected by biases (Lipsitch et al., 2015), above all in the growing phase of the epidemic, when the number of hospitalisations increases more steeply (Seaman et al., 2022; Seaman, Presanis, and Jackson, 2022). Some corrections have been proposed, but they assume the availability of further information, either about the time series of people recovered and discharged from hospital (Yip et al., 2005; Yip and Huggins, 1995) or about the distribution of the delay between hospitalization and death or recovery (Ghani et al., 2005; Overton et al., 2022).

This information is not likely to be available early in an outbreak, especially when a new pathogen emerges. For this reason it seems feasible to rethink this problem in a SSM context and integrate over the information that is not available.

2.2 A state-space model for hCFR

Our SSM should describe individuals staying and leaving the hospital as time elapses. Let X_t, Y_t and Z_t denote the number of people that remain in hospital, die and recover (hence discharged) respectively during interval t . Moreover, let h_t denote the number of individuals entering the hospital at time t ; h_t is assumed fixed and known.

Let $\theta = (p_H, p_D, p_R)$ denote the static parameters, where p_H, p_D and p_R are the probability of remaining in hospital, dying and recovering (and being discharged) within the interval considered (e.g. a week), respectively. Note that θ is subject to the constraint $p_H + p_D + p_R = 1$.

The state process modelling the individuals staying in the hospital, dying and recovering can be expressed with the following chain Multinomial model:

$$(X_t, Y_t, Z_t | x_{t-1}, h_{t-1}) \sim \text{Multinomial}(x_{t-1} + h_{t-1}, \theta). \quad (1)$$

As mentioned above, the number of individuals dying is very often closely monitored. Therefore, we assume that the deaths are fully observed and consider Equation (1) as defining both the state and observation process. The state process at time $t = 0$ depends on the disease under analysis and the monitoring system used. Since h_0 , and every hospitalization before the start of the monitoring system, is not recorded, X_0 encapsulates all the individuals that were still in the hospital before the beginning of the data-collection. X_0 , for the example of seasonal influenza, can be assumed to take non negative values, for example defining the prior distribution:

$$X_0 \sim \text{Poisson}(1.5). \quad (2)$$

The system is illustrated by the directed acyclic graph (DAG) in Figure 1, where a further node $IC_t = h_t + x_t$ has been introduced to clarify the size of the Multinomial r.v., i.e. the number of individuals in hospital at the start of the t th time interval.

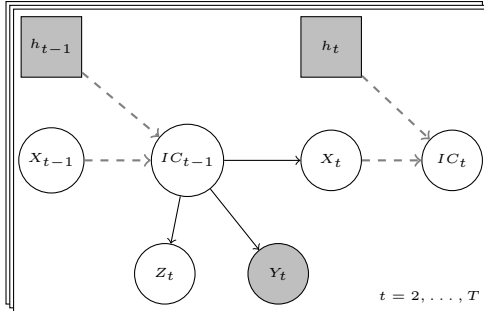


Figure 1: DAG describing the SSM of Equation 1. Dashed arrows represent deterministic relationships and solid arrows stochastic relationships; white circles represent unknowns and grey boxes represent observed quantities, squares are assumed fixed while circles are assumed to distribute according to the observation process.

While the time series $\mathbf{y}_{1:T}$ and $\mathbf{h}_{1:T}$ are known, we assume no observations on $\mathbf{x}_{0:T}$ ($\mathbf{z}_{1:T}$ follows from knowing $\mathbf{x}_{0:T}$). In Section 2.3 below, we propose a particle filter that samples from the filtering distribution $p(\mathbf{X}_{1:t} | \mathbf{y}_{1:t}, \theta)$ for $t = 1, \dots, T$ and provides an estimate of the likelihood $\hat{p}(\theta | \mathbf{y}_{1:T})$.

2.3 A particle filter for θ

In this Section we present a commonly used particle filter, based on the construction of the bootstrap particle filter (BPF), that has a weakness that we will later address; this algorithm

aims to sample from the filtering distribution at each time point $t = 1, \dots, T$. This algorithm starts from an equally weighted sample from the filtering distribution at the previous time point $\{x_{t-1}^{(n)}\}_{n=1}^N$ and uses the state distribution as an importance distribution. The proposed particles $\{x_t^{(n)}\}_{n=1}^N$ are then accepted with weight proportional to the observation density at time t : $w_t^{(n)} \propto p(y_t | x_t^{(n)}, \theta)$, for $n = 1, \dots, N$. The mean of these un-normalised weights provides an approximation of the marginal likelihood of the parameter θ :

$$\widehat{p}(y_{1:T} | \theta) = \prod_{t=1}^T \frac{1}{N} \sum_{n=1}^N w_t^{(n)}.$$

The BPF bases the choice of its importance distribution on the prior knowledge of the SSM, and conditions on the parameter value θ that is currently being considered. This proposal, not being conditional to the data, might not match the filtering distribution well.

Since y_t is available at time t , and our target distribution is conditional on y_t , a better importance distribution could be given by $p(x_t | x_{t-1}, y_t, \theta)$, which takes into account the next available observation. Given system (1), conditionally on the number of people dying at time t , y_t , and on the people currently in hospital $x_{t-1} + h_{t-1}$, the number of people remaining in hospital x_t , is a Binomial r.v. with size $x_{t-1} + h_{t-1} + y_t$ and probability $p_H / (1 - p_D)$.

Algorithm 1 describes the particle filter obtained when the importance distribution at each time t is given by:

$$q_t(x_t | y_t, x_{t-1}, \theta) \sim \text{Binomial} \left(x_{t-1} + h_{t-1} + y_t; \frac{p_H}{1 - p_D} \right). \quad (3)$$

At each time step, a particle set of size N is proposed according to (3), each particle is then assigned un-normalised weight $w_t^{(n)} = \frac{p(x_t^{(n)}, y_t, z_t^{(n)} | x_{t-1}^{(n)})}{q(x_t^{(n)} | y_t, x_{t-1}^{(n)})}$, with $p(\cdot)$ being the state-observation density and $q(\cdot)$ the importance density; these weights contribute to the approximation of the likelihood of the parameter θ .

In this first application of SMC techniques to our low-valued discrete SSM, some pitfalls start appearing. The particle-swarm is directed to target the filtering distribution, accounting for the value of the current observation, y_t ; nevertheless, the chained nature of the system is such that the same particles that should be the most compatible with the observation y_t might also be incompatible with future outcomes y_{t+1}, y_{t+2}, \dots .

Since the distributions are discrete and on constrained spaces, this means that the size parameter of the Multinomial can be lower than a realisation (i.e., the observation). This incompatibility is likely to happen, for example, when estimating the likelihood of a parameter value θ , that is far from the true value. Figure 2 shows the particles proposed and resampled with Algorithm 1. Particle collapse is caused by the fact that, for all 500 particles, the number of people remaining in hospital at time $t = 14$, X_{14} , is smaller than the observation at that time.

An algorithm such as the alive particle filter (APF) would only try and overcome this particle-collapse problem via brute force, without really addressing the issue of an importance distribution that, while wisely chosen, is not robust enough to allow for outliers. This motivates the creation of a mechanism to sample from the filtering distribution that goes beyond the intensive use of the importance distribution (3).

Algorithm 1: Particle filter exploiting y_t .

input : $y_{1:T}$; $\theta = (p_H, p_D, p_R)$; N
output: an approximation of the likelihood $\hat{p}(y_{1:T}|\theta)$

for $n = 1, \dots, N$ **do**
 $x_0^{(n)} \sim \text{Pois}(1.5)$
 $w_0^{(n)} = \frac{1}{N}$ set the weights
 $x_1^{(n)} \sim \text{Binom}\left((x_0^{(n)} + h_0 - y_1); \frac{p_H}{1 - p_D}\right)$ propagate
 $w_1^{(n)} = \frac{p(x_1^{(n)}, y_1, z_1^{(n)} | x_0^{(n)})}{q(x_1^{(n)}, y_1 | x_0^{(n)})}$ compute the weights
end
 $\tilde{w}_1^{(n)} = \frac{w_1^{(n)}}{\sum_{n=1}^N w_1^{(n)}}$ normalise the weights
 $\{x_{0:1}^{(n)}, \tilde{w}_1^{(n)}\}_{n=1}^N$ approximation of the target
for $t = 2, \dots, T$ **do**
 for $n = 1, \dots, N$ **do**
 $x_{0:t-1}^{(n)} \sim \mathcal{C}\{x_{0:t-1}^{(j)}, \tilde{w}_{t-1}^{(j)}\}_{j=1}^N$ resample
 $x_t^{(n)} \sim \text{Binom}\left((x_{t-1}^{(n)} + h_{t-1} - y_t), \frac{p_H}{1 - p_D}\right)$ propagate
 $w_t^{(n)} = \frac{p(x_t^{(n)}, y_t, z_t^{(n)} | x_{t-1}^{(n)})}{q(x_t^{(n)}, y_t | x_{t-1}^{(n)})}$ compute the weights
 end
 $\tilde{w}_t^{(n)} = \frac{w_t^{(n)}}{\sum_{n=1}^N w_t^{(n)}}$ normalise the weights
 $\{x_{0:t}^{(n)}, \tilde{w}_t^{(n)}\}_{n=1}^N = \{x_{0:t-1}^{(n)}, x_t^{(n)}, \tilde{w}_t^{(n)}\}_{n=1}^N$ approximation of the target
end
approximate the likelihood by $\hat{p}(y_{1:T}|\theta) = \prod_{t=1}^T \frac{1}{N} \sum_{n=1}^N w_t^{(n)}$

3 The Lifebelt Particle Filter

3.1 The lifebelt particle

In the example presented in Section 2, there is a clear definition of the boundary of the state process. The upper limit of the state process is determined by the situation when no one leaves the hospital except for the observed individuals that die, $(y_{1:T})$. If this is the case the state process $\mathbf{X}_{1:T}$ takes its highest possible value at each time step.

A rule can be set to obtain a realisation of this specific trajectory that delimits the boundary of the state-space:

$$\begin{cases} x_t &= x_{t-1} + h_{t-1} - y_t \\ y_t &= y_t \\ z_t &= 0 \end{cases} \quad (4)$$

This trajectory has the special characteristic that it cannot collapse to zero weight, since, not only does it guarantee that the number x_t remains higher than the current observation y_t , but it takes its highest possible value, preventing future collapses due to the constrained space of the Multinomial.

The LBPF is based on the introduction of this trajectory, the *lifebelt particle*, in the sequential importance sampling algorithm. The particle takes its name from the fact that, in situations where all the other particles have weight 0, the lifebelt particle would still retain a positive weight, hence rescuing the overall sequential importance sampler from particle collapse. It is

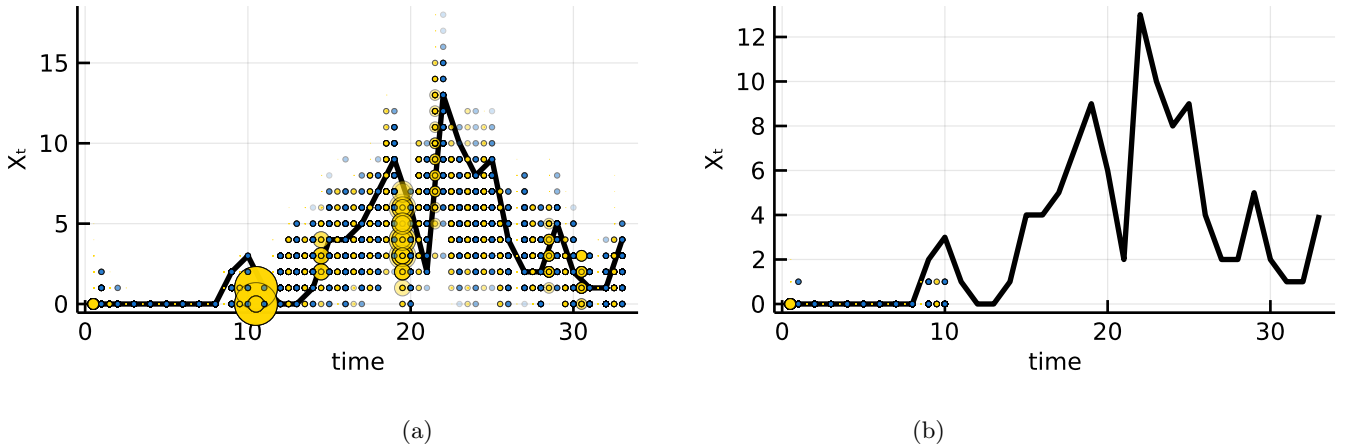


Figure 2: Particle swarm over time (x-axis) of one application of Algorithm 1 to data generated with parameters $\theta = (0.1, 0.8, 0.1)$, with $N = 500$, for estimating the likelihood of (a) the parameters generating the data and (b) a value in the tail: $\theta = (0.01, 0.6, 0.39)$. The black line in the background is the true, unknown, value of the latent state $\mathbf{x}_{1:T}$; the yellow dots are the samples drawn from the importance distributions at each time step, their size is proportional to the normalised weight; the equally-sized blue dots are the resampled particles.

important to note that this lifebelt particle is also safe against particle collapse generated by values of the hidden states that are too low compared to the observations.

Equation 4 provides an example of how one such particle can be formulated. More choices of lifebelt particles are discussed in Section 3.3 and 5. The remainder of this section is focused on the construction of an exact SMC scheme that includes a lifebelt particle.

3.2 The LBPF algorithm

The LBPF however, aims at being more robust than traditional sequential importance sampling with resampling (SIRS) and sequential importance sampling (SIS) schemes, thanks to the joint effect of two safety measures.

The first safety measure consists of the inclusion of one (or more) *lifebelt particle(s)* in the the particle swarm. This particle has the particular characteristic of defining the boundaries of the possible latent process, hence guaranteeing a positive weight. The definition of the lifebelt particle is clearly problem specific (as presented in the examples below). The lifebelt particle is included in the overall particle swarm by the sequential use of deterministic mixture importance sampling (DMIS) outlined in Section 3.2.1.

The second safety measure is that this lifebelt particle does not go through a resampling step. While all other particles get regenerated via resampling, the lifebelt particle is always retained and deterministically moved to the next time-step, allowing the sample to always have at least that one particle with positive weight. The combination of the main particle swarm with the lifebelt particle is illustrated in Section 3.2.2. These steps allow the main particle swarm to be formulated so that it best targets the distribution of interest (e.g. using information on y_t): no other particle but the lifebelt particle is wasted on the boundary of the latent state but whenever the main particle swarm collapses, for example due to an outlier, the lifebelt particle can be resampled and carried on until the end of the run of the filter.

3.2.1 Deterministic mixture importance sampling and its sequential use

DMIS was introduced by Owen and Zhou (2000) and later exploited in Cornuet et al. (2012). In its static version, we are interested in a target distribution X , whose probability density function (p.d.f.) can be evaluated up to a normalising constant $\pi(x) = \frac{f(x)}{\gamma}$ but from which we cannot directly sample. Samples from X can be obtained by importance sampling, where the importance distribution $q(x)$ is defined as a deterministic mixture distribution.

$$\begin{aligned} x^{(n)} &\sim q_1 && \text{for } n = 1, \dots, N_1 \\ x^{(n)} &\sim q_2 && \text{for } n = N_1 + 1, \dots, N_1 + N_2 \\ &\dots && \\ x^{(n)} &\sim q_G && \text{for } n = \sum_{g=1}^{G-1} N_g + 1, \dots, N \end{aligned}$$

with $N = \sum_{g=1}^G N_g$. Owen and Zhou (2000) propose to pool the samples together recomputing the weights as if the total sample was drawn from a mixture of all the densities $q_1(x), q_2(x), \dots, q_G(x)$: $q(x^{(n)}) = \frac{1}{N} \sum_{g=1}^G N_g q_g(x^{(n)})$ resulting in the deterministic mixture weight:

$$w^{(n)} = \frac{f(x^{(n)})}{\frac{1}{N} \sum_{g=1}^G N_g q_g(x^{(n)})} \quad (5)$$

Despite the importance samples not being drawn from a mixture distribution, these weights allow exact Monte Carlo (MC) estimation (see derivation Cornuet et al., 2012).

Cornuet et al. (2012) underlines that the samples obtained are a valid importance-sampling approximation for the target $\pi(x)$ if every sub-sample of size N_g is a valid importance sample, i.e. if the support of q_g contains the support of $\pi(x)$. In this case, the DMIS can be seen as a method that simply *pools* importance-sample estimators obtained from many different importance distributions. We extend this here by noting that if the support of the target density Ω , can be covered jointly by the q_g s: i.e. $\text{supp}(q_g) = \Omega_g$, for $g = 1, \dots, G$, with $\Omega \subseteq \bigcup_{g=1}^G \Omega_g$, then this importance sample retains exactness (see derivation in Appendix A).

It is now clear that the DMIS can be used to combine one or more lifebelt particles with one or more remaining particle swarms by the sequential use of a deterministic mixture, where one component of the mixture moves according to the lifebelt particle dynamics.

3.2.2 Combination of non-resampled and resampled particle sets

A problematic task that arises when attempting to include the lifebelt particle in another particle filter is that, not only should the importance distribution at each time step be formulated as a DMIS, but also the lifebelt particle trajectory should be followed sequentially over time, and therefore must be protected from disappearing in the resampling sampling.

The weight presented in Equation (5) needs to be further corrected to account for this merge of a set of particles drawn with SIRS and another, the lifebelt, drawn with SIS without resampling.

To do so, we consider the case where only these two samplers are combined, this can easily be extended to more than two samplers, some of which are resampled and others that aren't. We construct the derivation of the weights of the target distribution.

Let N_r denote the number of particles that go through resampling and N_s the number of particles that are carried on throughout the particle filter. Let $N = N_r + N_s$ denote the total number of particles. Assume that at time $t - 1$ the set $\left\{x_{t-1}^{(n)}; w_{t-1}^{(n)}\right\}_{n=1}^N$ is a weighted sample

from the target distribution, i.e. the filtering distribution $p(\mathbf{X}_{t-1}|\mathbf{y}_{1:t-1}, \boldsymbol{\theta})$, where $w_{t-1}^{(n)}$ are un-normalised weights, available from the weighting step.

Given normalised weights $\tilde{w}_{t-1}^{(n)} = \frac{w_{t-1}^{(n)}}{\sum_{n=1}^N w_{t-1}^{(n)}}$, an equally-weighted sample of size N_r from $p(\mathbf{X}_{t-1}|\mathbf{y}_{1:t-1}, \boldsymbol{\theta})$ can be obtained, for example, by Multinomial resampling:

$$\mathbf{x}_{t-1}^{(n)} \sim \mathcal{C} \left\{ \mathbf{x}_{1:t-1}^{(j)}, \tilde{w}_{t-1}^{(j)} \right\}_{j=1}^N \quad \text{for } n = 1, \dots, N_r.$$

This will compose the SIRS part of the particle swarm. Note that here the sample is taken from the whole particle set: the lifebelt particle, which will be in the set of size N_s , always resampled, is allowed to be picked among the N_r particles. The remaining N_s particles are not resampled.

Once the desired particle swarm is available, the DMIS helps to progress differently the two sets of particles. Let $q(x)$ denote the form of the importance density which, for the DMIS, is $q(x) = \frac{1}{N} \sum_{g=1}^G N_g q_g(x)$. A new set of proposed particles $\{x_t^{(n)}\}_{n=1}^N$ is obtained. The weights at time t , which can be used to approximate the marginal likelihood of the parameter $\boldsymbol{\theta}$, are then:

$$w_t^{(n)} = \begin{cases} \frac{p(y_t, x_t^{(n)} | x_{t-1}^{(n)}, \boldsymbol{\theta})}{q(x_t^{(n)})} & \text{for } n = 1, \dots, N_r \\ \frac{p(y_t, x_t^{(n)} | x_{t-1}^{(n)}, \boldsymbol{\theta})}{q(x_t^{(n)})} \tilde{w}_{t-1}^{(n)} & \text{for } n = N_r + 1, \dots, N_r + N_s \end{cases} \quad (6)$$

These weights could then be self-normalised s.t. $\tilde{w}_t^{(n)} = \frac{w_t^{(n)}}{\sum_{n=1}^N w_t^{(n)}}$

3.3 Algorithm specification and pseudo-code

Algorithm 2 reports the general form of the LBPF. Here the importance distribution is simply denoted by q , which comprises the deterministic mixture of the G components, some of which go through resampling and some of which do not. It is clear that the lifebelt particle(s) must be among the N_s particles that do not go through resampling.

This algorithms provides an estimate of the likelihood of the data $y_{1:T}$ given a specific parameter value $\boldsymbol{\theta}$.

Note that in Algorithm 2 N_s can be larger than 1 allowing for multiple lifebelt particles. These particles are always resampled until the end of the time series. While some of them might not be completely safe against particle collapse (e.g. allowing the possibility of zero-weights) by construction, it might be useful to introduce them to populate some areas of the hidden space that would otherwise remain uncovered (see example in Section 4.3).

4 Application of the LBPF to the hospitalisation-death model

A natural specification for a specific lifebelt particle for the model in Figure 1 was provided in Equation (4). In this section we implement the LBPF, firstly including a single particle formulated as in (4), then providing an improved version that has multiple lifebelt particles. Lastly we specify a full pseudo-marginal algorithm that uses a LBPF to approximate the likelihood of a specified parameter value $\boldsymbol{\theta}$ in the acceptance step of a MH algorithm.

Algorithm 2: Lifebelt Particle filter

input : $\mathbf{y}_{1:T}; \boldsymbol{\theta}; N_r; N_S; q_r; q_s; p(x_0)$.
output: an approximation of the likelihood $\hat{p}(\mathbf{y}_{1:T}|\boldsymbol{\theta})$.

for $n = 1, \dots, N_r$ **do**
 | $x_0^{(n)} \sim \text{Poisson}(1.5)$ sample the state in 0 from the prior
end
for $N_r + 1, \dots, N$ **do**
 | $x_0^{(n)} \sim q_s(x_0|\mathbf{y}_{1:T})$ sample/set the state in 0 for the lifebelt particle
end
 $\tilde{w}_0^{(n)} = \frac{1}{N}$ initialise the weights
for $t = 1, \dots, T$ **do**
 | **for** $n = 1, \dots, N_r$ **do**
 | $x_{0:t-1}^{(n)} \sim \mathcal{C}\left\{x_{0:t-1}^{(j)}, \tilde{w}_{t-1}^{(j)}\right\}_{j=1}^N$ resample
 | $x_t^{(n)} \sim q_r\left(x_t|x_{t-1}^{(n)}, y_t\right)$ propagate
 | $w_t^{(n)} = \frac{p(x_t^{(n)}, y_t|x_{t-1}^{(n)})}{q(x_t^{(n)}|x_{t-1}^{(n)}, y_t)}$ compute the weights
 | **end**
 | **for** $n = N_r + 1, \dots, N$ **do**
 | $x_{0:t-1}^{(n)} = \left\{x_{0:t-1}^{(n)}, \tilde{w}_{t-1}^{(n)}\right\}$ propose the lifebelt trajectories
 | $x_t^{(n)} \sim q_i\left(x_t|x_{t-1}^{(n)}, y_t\right)$ propagate
 | $w_t^{(n)} = \frac{p(x_t^{(n)}, y_t|x_{t-1}^{(n)})}{q(x_t^{(n)}|x_{t-1}^{(n)}, y_t)} \cdot \tilde{w}_{t-1}^{(n)}$ compute the weight
 | **end**
 | $\tilde{w}_t^{(n)} = \frac{w_t^{(n)}}{\sum_{n=1}^N w_t^{(n)}}$ for $n = 1, \dots, N$ normalize the weights
 | $\left\{x_{0:t}, w_t^{(n)}\right\}_{n=1}^N = \left\{x_{0:t-1}, x_t^{(n)}, w_t^{(n)}\right\}_{n=1}^N$ approximation of the target
end
approximate the likelihood by $\hat{p}(\mathbf{y}_{1:T}|\boldsymbol{\theta}) \approx \prod_{t=1}^T \frac{1}{N} \sum_{n=1}^N w_t^{(n)}$

4.1 Specification of the LBPF for the estimation of $\boldsymbol{\theta}$

We consider the combination of $N - 1$ particles drawn according to the importance distribution (3) and 1 lifebelt particle. The DMIS has then two components:

1. $x_t^{(n)} \sim q_1(x_t^{(n)})$ is the Binomial distribution that is obtained conditionally on the number of deaths at time t , y_t , being available:

$$x_t^{(n)}|x_{t-1}^{(n)}, y_t \sim \text{Binomial}\left(\left(x_{t-1}^{(n)} + h_{t-1} - y_t\right), \left(1 - \frac{p_R}{1 - p_D}\right)\right)$$

for $n = 1, \dots, N_1$

2. $x_t^{(n)} \sim q_2(x_t^{(n)})$ is a Dirac point mass distribution centred in the *lifebelt* case where all the people who enter the hospital and do not die stay in the hospital:

$$x_t^{(n)}|x_{t-1}^{(n)}, y_t \sim \delta_{x_{t-1}^{(n)} + h_{t-1} - y_t}(x) \quad (7)$$

where the $n = N_1 + 1$ is a unique particle: $N_2 = 1$

The importance distribution q_2 is what generates the *lifebelt* particle, which is ensured to have always positive weight, hence it will not be resampled but always progressed. An example of the proposed and accepted particles are displayed in Figure 3.

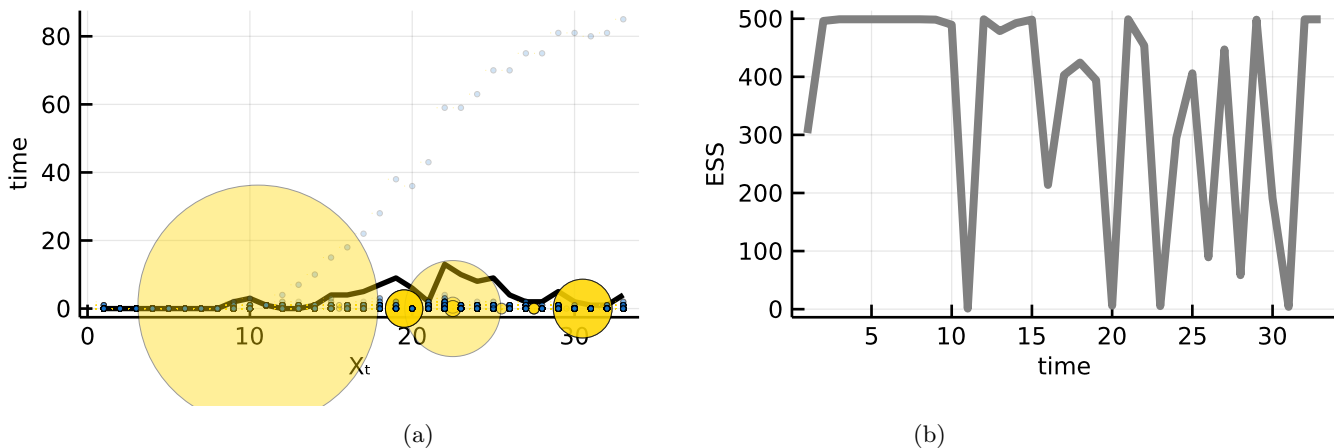


Figure 3: (a) Particle swarm of one application of Algorithm 1 with $N = 500$, for estimating the likelihood of the parameter $\theta = (0.01, 0.6, 0.39)$, applied to data generated with parameter $\theta = (0.1, 0.8, 0.1)$. The black line in the background is the true, unknown, value of the latent state $\mathbf{x}_{1:T}$; the yellow dots are the samples drawn from the importance distributions at each time step, their size is proportional to the normalised weight; the equally-sized blue dots are the resampled particles. (b) ESS of the particles over time.

Furthermore, we run checks to assess that the introduction of such a peculiar particle does not bias the estimation of the likelihood which should be kept unbiased by the new computation of the rates as illustrated in Section 3. The profile likelihood estimated with and without the lifebelt particle are not clearly distinguishable (figure reported in the Supplementary Information).

4.2 The lifebelt fleet: a richer LBPF

Note that this algorithm is flexible to many variations. We have presented a specific LBPF where only one particle follows a non-resampling dynamics. Another proposal could be to have more than one lifebelt particle and allocate them so that all the upper tail of the hidden process is covered. For example one could start with $T + 1$ particles in the lifebelt location, where T is the length of the time series modelled. At each time point one of the $T + 1$ particles that were in the lifebelt location starts following the dynamics of the main particle swarm. These particles can be visualised in Figure 4.

This would mean introducing a further importance density to the DMIS proposed in Section 4.1:

3. $x_t^{(n)} \sim q_3(x_t^{(n)})$ depends on time and it is different for each particle: as the particle index n increases, the particle will stop following q_2 and follow q_1 instead.

Let $k = n - N_1 - N_2 + 1$

$$\begin{cases} x_t^{(n)} | x_{t-1}^{(n)}, y_t \sim \delta_{x_{t-1}^{(n)} + h_{t-1} - y_t}(x) & \text{if } k < t \\ x_t^{(n)} | x_{t-1}^{(n)}, y_t \sim \text{Binomial}\left(n = (x_{t-1}^{(n)} + h_{t-1} - y_t), p = \left(1 - \frac{p_R}{1 - p_D}\right)\right) & \text{if } k \geq t \end{cases}$$

where $n = N_1 + N_2 + 1, \dots, N_1 + N_2 + N_3$ with $N_3 = T$.

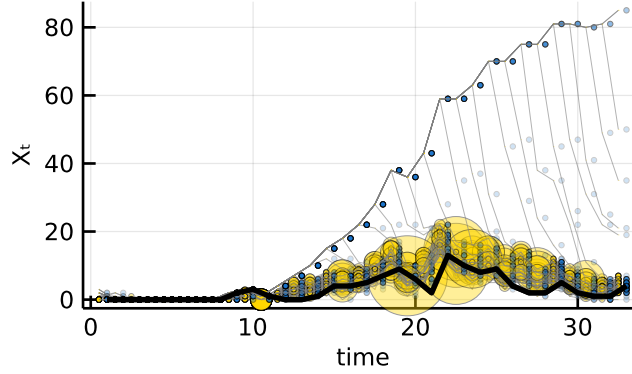


Figure 4: Particle swarm obtained by the use of $T + 1$ lifebelt particles, one of which follows deterministic dynamics given by (7), and the remaining T initially follow the dynamics (7), and as time progresses rejoin the main particle swarm. The thick black line is the true, unknown, value of the latent state $\mathbf{x}_{1:T}$; the yellow dots are the samples drawn from the importance distributions at each time step, their size is proportional to the normalised weight; the equally-sized blue dots are the resampled particles. The trajectories are connected by grey lines according to the particle indices.

The choices of how to formulate DMIS are problem-dependent and should be tailored to the hidden space under analysis. The advantage of a particle filter constructed under these rules is that the amount of particles employed for some particular tasks (e.g. sampling from the boundaries or the tails of the latent space) are specified. Differently from algorithms like the APF, the computations have always an upper bound and the statistician is free to decide where to target their computational resources.

The reason for choosing multiple lifebelt particles is also the fact that, in case one of the lifebelt particles is resampled, if all other particles fail, its weight might be very small. This is due both to the fact that (a) the lifebelt particle often represents an extreme scenario, and (b) its weight is decreasing quickly as it does not go through resampling. Multiple lifebelt particles might allow us to cover the latent space better and retain less extreme particle trajectories. Note that, even with the use of the LBPF, the approximation of the log likelihood can be $-\infty$, due to numerical precision error, in which case this means that effectively the parameter of which we are evaluating the likelihood is not supported by the data. The LBPF allows a better approximation of the tails of the likelihood than other particle filtering methods.

4.3 Use of the LBPF in a pseudo marginal method

The LBPF provides an estimate of the likelihood of the data $\mathbf{y}_{1:T}$ given a specific value of the parameter vector $\boldsymbol{\theta}$. For this reason it can be used within a pseudo-marginal method (Andrieu

and Roberts, 2009). Here, among the available pMCMC methods, we chose to use grouped independence Metropolis Hastings (GIMH).

To explore $\theta = (p_H, p_D, p_R)$, the parameter space was transformed to lie in \mathbb{R}^2

$$\begin{aligned}\gamma_1 &= \text{logit}\left(\frac{p_D}{p_D + p_R}\right) \\ \gamma_2 &= \text{logit}(p_D + p_R)\end{aligned}\tag{8}$$

with inverse:

$$\left(\frac{e^{\gamma_1 + \gamma_2}}{(1 + e^{\gamma_1})(1 + e^{\gamma_2})}, \frac{e^{\gamma_2}}{(1 + e^{\gamma_1})(1 + e^{\gamma_2})}\right)\tag{9}$$

A Dirichlet(1,1,1) was assumed on the simplex of θ , granting a uniform prior. A dataset was generated with a specific parameter set $\theta = (p_H = 0.3, p_D = 0.5, p_R = 0.2)$. An MCMC was run: convergence is fast and the chains show good mixing (see Figure 5 below).

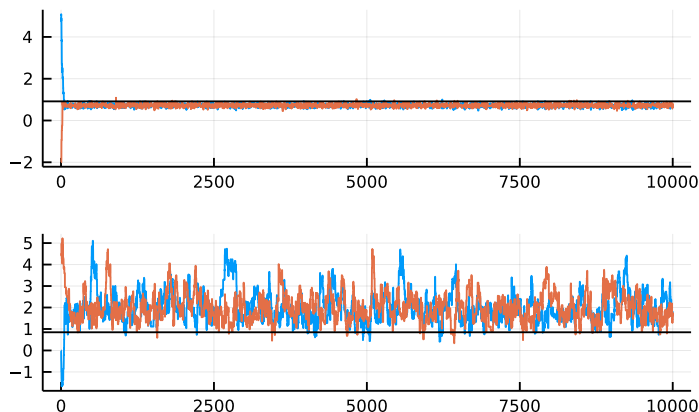


Figure 5: pMCMC with likelihood estimated by Algorithm 2.

Compared to the standard pMCMC that adopts Algorithm 1 for the estimation of the likelihood, there is no apparent difference in the chain and, as expected, no bias is introduced in the posterior inference (see comparison plot in the Supplementary Information).

5 Comparison with Alive Particle Filter

In this section we assess whether the LBPF presented in Section 4.1 with $N = 500$ total particles does indeed cut the computation time compared to the APF.

We implemented a version of the APF that uses as importance distribution Equation (3). Moreover we consider a target number of non-zero-weighted particles of $N = 500$, and we bound the number of proposals at each time point to be $n_t \leq 1$ million, i.e., when 500 non-zero-weighted particles are not obtained by the 1 millionth attempt, the filter proceeds to the next time step resampling only among the simulated particles, if any of these has a weight larger than 0.

We analyse a simulated dataset, generated with parameter set: $\theta = (p_H = 0.3, p_D = 0.5, p_R = 0.2)$. This dataset presents some challenges as there are many spikes in the unknown number of people remaining in hospital, which might be difficult to be matched by the importance density.

While the chain in practice looks very similar to the one obtained with the LBPF, the MCMC using APF takes 30% to 50% more time than the MCMC that uses the LBPF. To understand why this is happening in practice we can look at the distribution of the total number of proposals over time $n = \sum_{t=1}^T n_t$ for the proposed parameter θ^* at each iteration of the MCMC; the histogram of this quantity over the 10,000 MCMC iterations is reported in Figure 6.

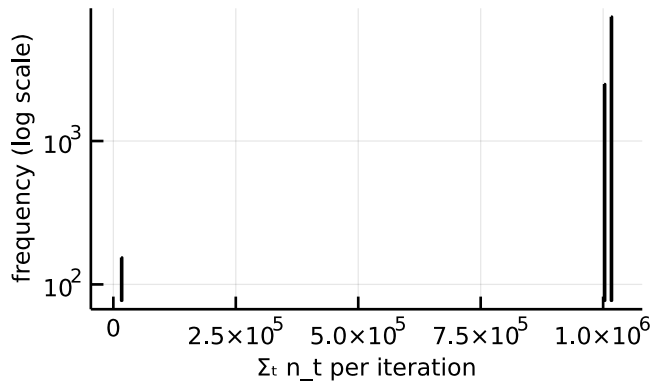


Figure 6: Histogram of the number of attempts made by the APF.

The small column to the left-hand side represents those MCMC iterations for which the APF obtains an estimate of the likelihood only using 500 particles per time point. The second column from the right, in the middle represents all those MCMC iterations for which the APF failed in its attempt, at some point $t < T$, to obtain any non-zero-weighted particles. The filter stopped at t and estimated the likelihood of the parameter proposed in that MCMC iteration to be zero. Lastly the highest column on the right-hand side represents all those MCMC iterations for which the APF managed to obtain at least one particle with non-zero weight, it continued to propose until the maximum limit of 1 million particles was reached, and then resampled those few non-zero-weighted particles to continue the filter until the end of the time series T .

If we compare this with the LBPF, we note that the latter always uses a constant number of particles (in this case fixed to 500). When the particles from the main filter do not manage to provide a good approximation of the filtering distribution, instead of insisting with the intensive use of an inadequate importance distribution, it samples the lifebelt particle, that is formulated to be more robust against particle failure.

Irrespective of the computation time, we could compare the quality of the likelihood approximation via LBPF vs via APF for each proposed value of the MCMC. This quality be assessed by computing the ESS of the particles used to approximate the likelihood. Figure 7 compares the ESS of the particle swarm used to approximate the value of the proposed value θ^* at each iteration of the MCMC. Both considering the ESS averaged across time points and the ESS of the particles at the final time point, LBPF seems to provide better estimates of the likelihood in terms of higher ESS. Unlike the APF, the LBPF does not have a mode at small ESS values where the particle filter collapses and the likelihood is estimated to be zero. Furthermore, it seems that when the lifebelt particle is actually used, this regenerates and enriches the particle swarm in the following time steps as noted in Section 4.

Note that these results refer to the specific scenario considered, which happens to be particularly challenging, rather than providing a general conclusions on the performance of the LBPF versus the APF. Moreover, we have used the basic formulation of the APF, without considering

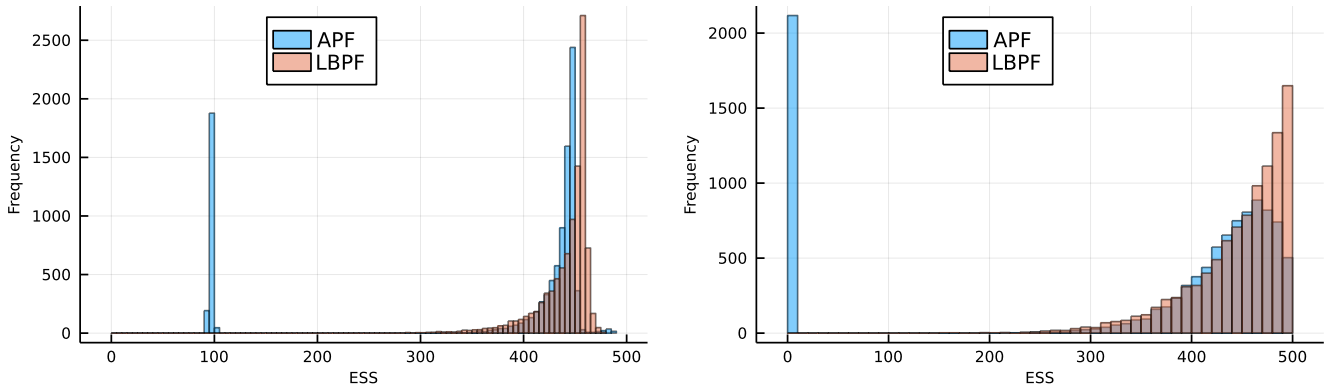


Figure 7: Comparison of the ESS of the particles averaged over time (left) and at the last time step (right) for the parameter proposed at each iteration of the MCMC run with APF and LBPF.

more complex/bespoke versions of this algorithm.

6 Discussion

In this paper we have proposed a new particle filter that combines a SIRS with a SIS without resampling whose importance distribution is chosen specifically to avoid particle failure. The algorithm relies on the introduction of a specific *lifebelt* particle, robust to particle collapse, whose formulation is problem specific.

We have presented the example of a SSM for hospital admissions and deaths in hospital where small counts and strong temporal dependence makes running a standard particle filter more challenging.

There are many other instances in which the LBPF could be used. For example, one could consider queue systems where entries, exits and waiting times are only partially monitored, here the lifebelt particle could be formulated according to a criteria similar to the one used for the deaths in hospital (i.e. covering the upper limit of the hidden state). Other examples could be taken from the inference of epidemic models (as in McKinley et al., 2020): here the individuals are divided into groups according to their disease status and observations are often made on the individuals leaving the infectious state. The lifebelt particle could be formulated by assuming that all the individuals who are eventually ill, become infectious soon after the epidemic has started and progressively move to the recovered/removed state. Lastly, the LBPF could also be extended to continuous SSMs. In this context the lifebelt particle could follow an over-dispersed importance distribution to protect against future shocks. While this does not guarantee absolute safety of the lifebelt particle, it may still be effective at preventing particle collapse in many cases. The extension to continuous SSM, however, would require a further analysis of exactness, since the proofs presented here are based on discrete r.v.s.

Our contribution, rather than providing a tool that can be blindly applied to any SSMs, offers a framework that can be used to combine different importance distributions, some of which might not be formulated to sample from the mass of the filtering distribution, but instead have the role of covering its tail. This framework becomes useful under a computational budget perspective: the resources are better shared between multiple candidate importance distributions. Moreover the proposed algorithm presents advantages also under the point of view of inferring the hidden

space: preserving particles that sample from the tails of the filtering distribution leads to a better estimate of the likelihood in terms of effective sample size. We have shown how the combination of multiple importance distributions is possible without biasing the likelihood estimator.

In addition to proposing this setup which helps in many other settings, the example presented of the estimation of CFR for hospitalised patients is of key relevance. At the beginning of the recent Covid-19 pandemic, only time series of cases and deaths were reported. Ratios of cumulative counts of cases and deaths provided biased estimates of the CFR: our particle filter approach instead integrates over what is unknown and, given the introduction of the lifebelt particle, is robust to data which might be unexpected.

Acknowledgements

AC, GOR, SEFS and DDA are supported by Bayes4Health EPSRC Grant EP/R018561/1. AC, AMP, PJB and DDA are supported by the MRC, programme grant MC_UU_00002/11. TJM is supported by an “Expanding Excellence in England” award from Research England. GOR is further supported by the Alan Turing Institute.

References

- Anderson, J. L. (1996). “A method for producing and evaluating probabilistic forecasts from ensemble model integrations”. In: *Journal of climate* 9.7, pp. 1518–1530.
- Andrieu, C., A. Doucet, and R. Holenstein (2010). “Particle markov chain monte carlo methods”. In: *Journal of the Royal Statistical Society: Series B (Statistical Methodology)* 72.3, pp. 269–342.
- Andrieu, C. and G. O. Roberts (2009). “The pseudo-marginal approach for efficient Monte Carlo computations”. In: *The Annals of Statistics* 37.2, pp. 697–725.
- Arulampalam, M. S., S. Maskell, N. Gordon, and T. Clapp (2002). “A tutorial on particle filters for online nonlinear/non-Gaussian Bayesian tracking”. In: *IEEE Transactions on signal processing* 50.2, pp. 174–188.
- Bretó, C., D. He, E. L. Ionides, and A. A. King (2009). “Time series analysis via mechanistic models”. In: *The Annals of Applied Statistics*, pp. 319–348.
- Chopin, N., P. E. Jacob, and O. Papaspiliopoulos (2013). “SMC2: an efficient algorithm for sequential analysis of state space models”. In: *Journal of the Royal Statistical Society: Series B (Statistical Methodology)* 75.3, pp. 397–426.
- Chopin, N., O. Papaspiliopoulos, et al. (2020). *An introduction to sequential Monte Carlo*. Springer.
- Cornuet, J.-M., J.-M. Marin, A. Mira, and C. Robert (2012). “Adaptive Multiple Importance Sampling”. In: *Scandinavian Journal of Statistics* 39.4, pp. 798–812.
- Del Moral, P., A. Jasra, A. Lee, C. Yau, and X. Zhang (2015). “The alive particle filter and its use in particle Markov chain Monte Carlo”. In: *Stochastic Analysis and Applications* 33.6, pp. 943–974.
- Doucet, A., A. M. Johansen, et al. (2009). “A tutorial on particle filtering and smoothing: Fifteen years later”. In: *Handbook of nonlinear filtering* 12.656-704, p. 3.
- Drovandi, C. C., A. N. Pettitt, and R. A. McCutchan (2016). “Exact and approximate Bayesian inference for low integer-valued time series models with intractable likelihoods”. In: *Bayesian Analysis* 11.2, pp. 325–352.

- Dukic, V., H. F. Lopes, and N. G. Polson (2012). “Tracking epidemics with Google flu trends data and a state-space SEIR model”. In: *Journal of the American Statistical Association* 107.500, pp. 1410–1426.
- Ghani, A. C., C. A. Donnelly, D. R. Cox, J. Griffin, C. Fraser, T. Lam, L. Ho, W. Chan, R. Anderson, A. Hedley, et al. (2005). “Methods for estimating the case fatality ratio for a novel, emerging infectious disease”. In: *American journal of epidemiology* 162.5, pp. 479–486.
- Gilks, W. R. and C. Berzuini (2001). “Following a moving target—Monte Carlo inference for dynamic Bayesian models”. In: *Journal of the Royal Statistical Society: Series B (Statistical Methodology)* 63.1, pp. 127–146.
- Gordon, N. J., D. J. Salmond, and A. F. Smith (1993). “Novel approach to nonlinear/non-Gaussian Bayesian state estimation”. In: *IEE proceedings F (radar and signal processing)*. Vol. 140. 2. IET, pp. 107–113.
- Griffin, A., P. A. Jenkins, G. O. Roberts, and S. E. Spencer (2017). “Simulation from quasi-stationary distributions on reducible state spaces”. In: *Advances in Applied Probability* 49.3, pp. 960–980.
- Health Protection Agency (2011). “Sources of UK flu data—Influenza Surveillance in the United Kingdom”. In: Available at the following link. URL: <https://webarchive.nationalarchives.gov.uk/ukgwa/20140713201509/http://www.hpa.org.uk/Topics/InfectiousDiseases/InfectionsAZ/SeasonalInfluenza/EpidemiologicalData/30influsourcesofUKfludata/>.
- Lipsitch, M., C. A. Donnelly, C. Fraser, I. M. Blake, A. Cori, I. Dorigatti, N. M. Ferguson, T. Garske, H. L. Mills, S. Riley, et al. (2015). “Potential biases in estimating absolute and relative case-fatality risks during outbreaks”. In: *PLoS neglected tropical diseases* 9.7, e0003846.
- McKinley, T. J., P. Neal, S. E. Spencer, A. J. Conlan, and L. Tiley (2020). “Efficient Bayesian model choice for partially observed processes: with application to an experimental transmission study of an infectious disease”. In: *Bayesian Analysis* 15.3, pp. 839–870.
- Overton, C. E., L. Webb, U. Datta, M. Fursman, J. Hardstaff, I. Hiironen, K. Paranthaman, H. Riley, J. Sedgwick, J. Verne, et al. (2022). “Novel methods for estimating the instantaneous and overall COVID-19 case fatality risk among care home residents in England”. In: *arXiv preprint arXiv:2202.07325*.
- Owen, A. and Y. Zhou (2000). “Safe and effective importance sampling”. In: *Journal of the American Statistical Association* 95.449, pp. 135–143.
- Schön, T. B., A. Svensson, L. Murray, and F. Lindsten (2018). “Probabilistic learning of nonlinear dynamical systems using sequential Monte Carlo”. In: *Mechanical systems and signal processing* 104, pp. 866–883.
- Seaman, S. R., T. Nyberg, C. E. Overton, D. J. Pascall, A. M. Presanis, and D. De Angelis (2022). “Adjusting for time of infection or positive test when estimating the risk of a post-infection outcome in an epidemic”. In: *Statistical methods in medical research* 31.10, pp. 1942–1958.
- Seaman, S. R., A. Presanis, and C. Jackson (2022). “Estimating a time-to-event distribution from right-truncated data in an epidemic: a review of methods”. In: *Statistical Methods in Medical Research* 31.9, pp. 1641–1655.
- Solin, A., M. Kok, N. Wahlström, T. B. Schön, and S. Särkkä (2018). “Modeling and interpolation of the ambient magnetic field by Gaussian processes”. In: *IEEE Transactions on robotics* 34.4, pp. 1112–1127.
- UK Health Security Agency (2021). “Sources of UK flu data—Influenza Surveillance in the United Kingdom”. In: Available at the following link. URL: <https://www.gov.uk/government/statistics/national-flu-and-covid-19-surveillance-reports-2021-to-2022-season>.

- World Health Organization (WHO) (2015). “A Manual for Estimating Disease Burden Associated with Seasonal Influenza.” In: p. 124. URL: http://www.who.int/influenza/resources/publications/manual_{_}burden_{_}of_{_}disease/en/.
- Yip, P. S., E. H. Lau, K. Lam, and R. M. Huggins (2005). “A chain multinomial model for estimating the real-time fatality rate of a disease, with an application to severe acute respiratory syndrome”. In: *American Journal of Epidemiology* 161.7, pp. 700–706.
- Yip, P. and R. Huggins (1995). “Some aspects of inference for chain binomial models”. In: *Stochastic Analysis and Applications* 13.3, pp. 355–367.

A Exactness of DMIS

To prove the exactness of DMIS with functions with different supports, we start from the proof of the exactness of DMIS. Let μ be the expected value of a function $h(X)$ where X is a r.v. with probability density function $f(x)$ ($\mu = \mathbb{E}[h(X)] = \int_{\Omega} h(x)f(x) dx$). Let $x^{(n)}$, for $n \in \left\{ \sum_{l=0}^{g-1} N_l + 1, \dots, \sum_{l=0}^g N_l \right\}$ (with $N_0 = 0$) be sampled from importance proposal q_g , for $g = 1, \dots, G$ and consider the estimator \hat{I} for μ :

$$\hat{I} = \frac{1}{N} \sum_{g=1}^G \sum_{n=1}^{N_g} h\left(x^{(n)}\right) \frac{f\left(x^{(n)}\right)}{\frac{1}{N} \sum_{l=1}^G N_l q_l\left(x^{(n)}\right)}$$

The expected value is:

$$\begin{aligned} \mathbb{E}[\hat{I}] &= \mathbb{E}\left[\frac{1}{N} \sum_{g=1}^G \sum_{n=1}^{N_g} h\left(x^{(n)}\right) \frac{f\left(x^{(n)}\right)}{\frac{1}{N} \sum_{l=1}^G N_l q_l\left(x^{(n)}\right)}\right] \\ &= \frac{1}{N} \sum_{g=1}^G \sum_{n=1}^{N_g} \mathbb{E}\left[h\left(x^{(n)}\right) \frac{f\left(x^{(n)}\right)}{\frac{1}{N} \sum_{l=1}^G N_l q_l\left(x^{(n)}\right)}\right], \quad \text{due to linearity of } \mathbb{E}. \end{aligned}$$

The N_g samples are drawn independent and identically distributed (iid) from the g -th importance distribution. DMIS assumes that each q_g is an appropriate importance distribution for f , i.e. $\Omega \subseteq \Omega_g$, the domain of f . Exactness, however, holds also if this is not the case.

$$\mathbb{E}[\hat{I}] = \frac{1}{N} \sum_{g=1}^G N_g \int_{\Omega_g} h(x) \frac{f(x)}{\frac{1}{N} \sum_{l=1}^G N_l q_l(x)} q_g(x) dx$$

Note that $f(x) = 0$ outside its support, i.e. in the set $\Omega_g \setminus \Omega$ and that $q_g(x) = 0$ outside Ω_g . Hence, we can add integrals that are equal to 0 to cover all the support Ω

$$\begin{aligned} &= \sum_{g=1}^G N_g \left[\int_{\Omega \cap \Omega_g} h(x) \frac{f(x)}{\sum_{l=1}^G N_l q_l(x)} q_g(x) dx + \underbrace{\int_{\Omega \setminus \Omega_g} h(x) \frac{f(x)}{\sum_{l=1}^G N_l q_l(x)} q_g(x) dx}_{=0} + \right. \\ &\quad \left. + \underbrace{\int_{\Omega_g \setminus \Omega} h(x) \frac{f(x)}{\sum_{l=1}^G N_l q_l(x)} q_g(x) dx}_{=0} \right] \\ &= \sum_{g=1}^G N_g \int_{\Omega} h(x) \frac{f(x)}{\sum_{l=1}^G N_l q_l(x)} q_g(x) dx \end{aligned}$$

Given that the integrals are all on the same support Ω we can bring the summation inside

$$\begin{aligned} &= \int_{\Omega} h(x) f(x) \sum_{g=1}^G N_g \frac{q_g(x)}{\sum_{l=1}^G N_l q_l(x)} dx \\ &= \int_{\Omega} h(x) f(x) dx = \mu \end{aligned}$$

(10)

and exactness of the estimator is proved.

Note that, while Cornuet et al. (2012) assumed that $\Omega \subseteq \Omega_g$ was a condition for exactness, this can be extended to the case where the G q_g s jointly cover the support of the target density, i.e. $\Omega = \bigcup_{g=1}^G \Omega_g$, while not containing it. In fact all the steps above are valid also while assuming $f(x) > 0$ in $\Omega - \Omega_g$ and $q_g(x) = 0$ in $\Omega - \Omega_g$